



Contents lists available at ScienceDirect

Journal of Asian Earth Sciences

journal homepage: www.elsevier.com/locate/jseas

Late Cenozoic tectonic deformation across the northern foreland of the Chinese Tian Shan

ChuanXin Li ^{a,b}, ZhaoJie Guo ^{a,*}, Guillaume Dupont-Nivet ^{a,c}

^a Key Laboratory of Orogenic Belts and Crustal Evolution, Ministry of Education, School of Earth and Space Sciences, Peking University, Beijing 100871, China

^b Research Institute of Petroleum Exploration & Development-Langfang, PetroChina, Langfang 065007, China

^c Paleomagnetic Laboratory, Faculty of Geosciences, Utrecht University, Budapestlaan 17, 3584 CD Utrecht, The Netherlands

ARTICLE INFO

Article history:

Available online xxx

Keywords:

Late Cenozoic
North Tian Shan
Foreland basin
Growth strata
Shortening rates

ABSTRACT

To understand the reactivation and intensified uplift of the Tian Shan range in the Cenozoic, the age of development of the associated series of anticlinal belts formed in the southern and northern foreland basins must be constrained. To estimate the shortening magnitude and rates in the northern foreland basin, we provide here regional structural analysis based on identified growth strata dated with existing magnetostratigraphy, together with balanced cross sections from interpreted seismic data. These results indicate that three paralleled rows of anticlinal belts have developed sequentially from south to north accommodating a total shortening of ~15 km at the location of the structurally restored seismic section provided here. These three belts present different structural deformational styles with the southern (Qingshuihe) anticline as a basement-involved fold, the middle (Huoerguosi) anticline as a fault-bend fold and the northern (Anjihai) anticline as a fault-propagation fold. Growth strata inferred from seismic profiles start stratigraphically far below growth strata observed on the outcrop. The latter coincide with accelerated folding of the anticlinal belts at ~6 Ma for the southern, ~2 Ma for the middle ~1 Ma for the northern. Our results imply that the northern Tian Shan foreland rates of deformation were lower until late Miocene and increased in more recent times to values in line with GPS-derived rates.

© 2010 Elsevier Ltd. All rights reserved.

1. Introduction

The Tian Shan orogenic belts (Fig. 1) provide an ideal setting to understand uplift, erosion and sedimentation processes and their relation to lithospheric deformation in response to the Indo-Asia collision (Molnar et al., 1993; Tapponnier and Molnar, 1979). As one of the best examples of active intracontinental orogenic systems, the Tian Shan has been the focus of a large number of geologic studies aiming in particular at constraining the age of the onset of deformation, the timing of the uplift and the rate of deformation and total associated convergence (Abdrakhmatov et al., 1996; Avouac et al., 1993). The continuous exposures of stratigraphic sequences found along the southern and northern forelands of the Tian Shan and the availability of sub-surface data from oil exploration seismic and well data, provide an ideal setting for constraining accurately in time the development of foreland structures associated to the range formation (Yin et al., 1998; Chen et al., 2007). To constrain the age of the stratigraphy, a large set of magnetostratigraphic studies have been conducted both on the northern and southern foreland basin sediments of the Tian Shan (Sun et al., 2004, 2007, 2008; Sun and Zhang, 2009; Charreau

et al., 2005, 2006, 2008; Huang et al., 2006; Heermance et al., 2007; Lu et al., 2010). While most of the structural studies have concentrated on the southern foreland of the Chinese Tian Shan (Yin et al., 1998; Bullen et al., 2001; Heermance et al., 2007), few integrated studies are focused on the northern foreland structural such that the regional context of the evolution and propagation of deformation remains poorly constrained quantitatively (Avouac et al., 1993; Avouac and Tapponnier, 1993). In this study, we provide regional structural analysis based on identified growth strata dated with published magnetostratigraphy, together with balanced cross sections from interpreted seismic data. These enable to estimate the shortening magnitude and rates of late Cenozoic structural deformations across the northern foreland of the Chinese Tian Shan.

2. Geological setting and stratigraphy

The ancestral Tian Shan is thought to have undergone two Paleozoic accretion events within paleo-Asia (Windley et al., 1990; Gao and Klemd, 2003; Shu et al., 2004; Li, 2006; Sobel et al., 2006; Xiao et al., 2009; Han et al., 2010). The first one, occurring in the Late Devonian–Early Carboniferous, along the southern margin of the range, resulted in the accretion of the central Tian Shan onto the Tarim block. The second one, occurring in the Late

* Corresponding author. Tel.: +86 10 62753545; fax: +86 10 62758610.

E-mail address: zjguo@pku.edu.cn (Z. Guo).

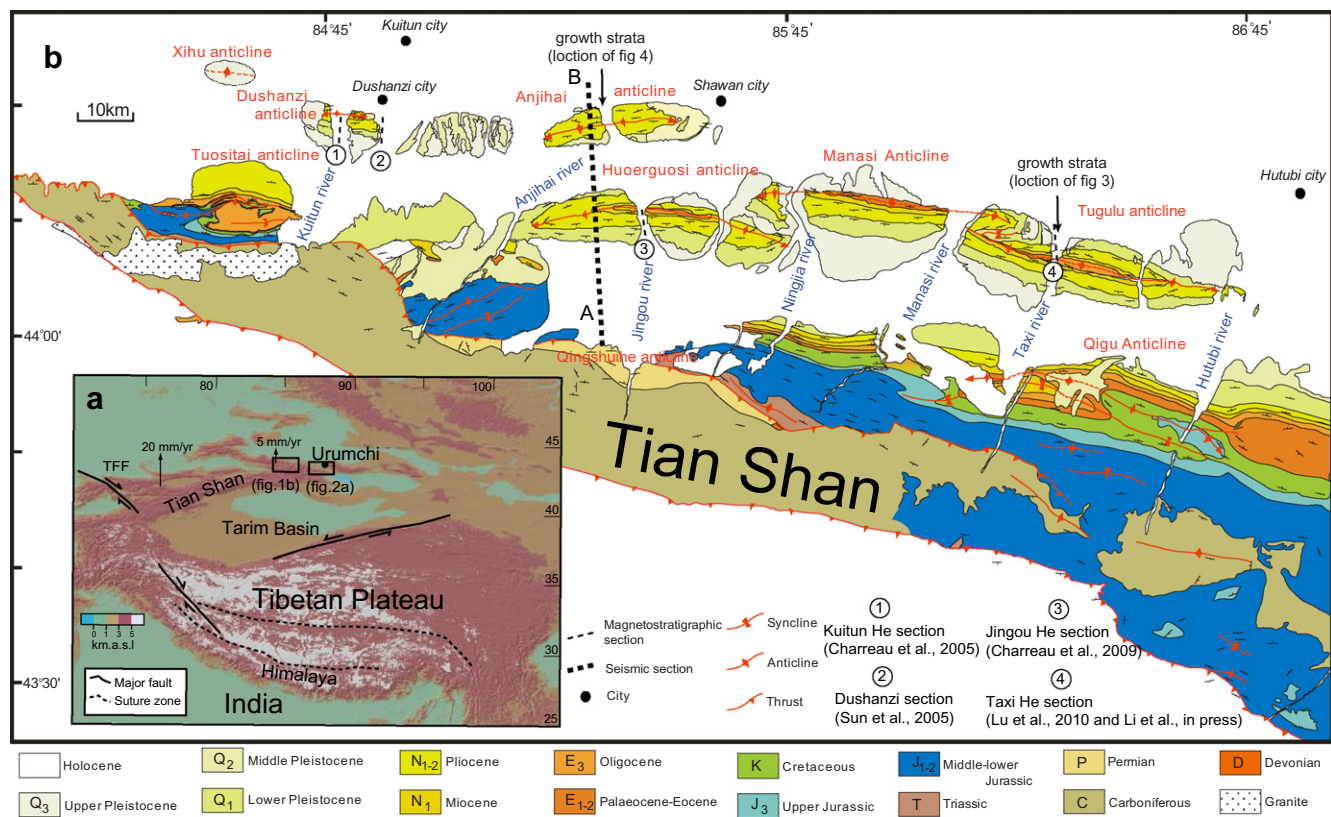


Fig. 1. Location and geologic setting of north Tian Shan. (a) Digital elevation model (GTOPO90) of the Indo-Asia collision zone. Arrows indicate GPS-derived shortening estimates (Abdrakhmatov et al., 1996; Wang et al., 2001). TFF: Talas Fergana Fault. (b) Schematic geologic map (modified from Deng et al., 2000) of the northern flank of the Tian Shan range including the location of sections sampled for chronostratigraphy from previous studies.

Carboniferous along the northern margin, led to the amalgamation of the Junggar block with the combined Tarim-central Tian Shan continental block. The present Tian Shan foreland is characterized by >10 km of Cenozoic strata deformed by Pleistocene detachment folds accommodating much of the recent shortening predicted by extrapolation of modern geodetic and Quaternary slip rates (Abdrakhmatov et al., 1996; Avouac et al., 1993; Scharer et al., 2006). The northern Tian Shan foreland is deformed by three recognized sets of east–west striking anticlinal belts (Deng et al., 2000) that are referred here (Fig. 1) as the southern belt (Tuositai–Qigu–Kalaza), the middle belt (Huoerguosi–Manasi–Tugulu) and the northern belt (Dushanzi–Anjihai). The orientation of these structures provides evidence for dominant north–south compression while the recurrence of these structures and the presence of faults on the north side of the anticlines suggest they are fault-propagation folds and/or fault-bend folds branching from a décollement layer at depth (Avouac et al., 1993).

Our study is focused on the north flank of the Chinese Tian Shan where the outcrop strata are mainly thick Cenozoic deposits that shed into the Junggar foreland basin from the south. Deformation on the middle belt exposes Paleogene lacustrine successions in the core of the anticlines to Plio–Pleistocene dipping fluvial and alluvial conglomeratic strata in the limbs (for detailed lithologic description and formation nomenclature, see Table 1). The Paleogene strata are mainly Lacustrine including the Ziniquanzi formation (E_{1-2z}), the Anjihai formation (E_{2-3a}) and the lower Shawan formation (E_3-N_1s). The Neogene strata are mainly composed of the fluvial Taxihe formation (N_{1t}) and Dushanzi formation (N_{1-2d}). The Quaternary strata are mainly alluvial massive gray poorly cemented conglomerate successions including the Xiyu formation (Q_{1x}) and the Wusu formation (Q_{2w}). These sediments have been dated at various sections along the strike of the northern Tian Shan

foreland structures yielding ages that are especially diachronous for the onset of the alluvial Xiyu formation (Charreau et al., 2008; Li et al., in press; Lu et al., 2010). Our structural analysis is based on a long N–S seismic profile (along the Jingou River) that includes the complete stratigraphy and cuts through the three structural belts (Fig. 1). To assess the timing of the structural deformation observed on this profile, we first review a regional investigation of growth strata across those three belts.

3. Syntectonic growth strata observations

Syntectonic growth strata are an effective marker of tectonic deformation in foreland basin (Suppe et al., 1992; Hardy and Poblet, 1994; Burbank et al., 1996). Because they are not apparent in outcrops along the Jingou river seismic profile for all of the three structural belts, we conducted detailed investigations of the geometry of syntectonic sediments along strike of the three parallel rows of anticline belts. Syntectonic growth strata were thus recognized at each row of the three belts. Together with the published age control from magnetostratigraphy, growth strata provide a record of the timing of tectonic deformation. It should be noted that the preserved growth strata provide a minimum age for the initiation of folding. Indeed, older growth strata, if ever present, could have occurred closer to the core of the fold but not have been preserved or not be visible on the outcrop. This will be discussed below in light of seismic profile analysis.

3.1. Growth strata in the southernmost belt

Detailed field investigations indicate that growth strata are present in the southernmost of the three belts at the Kalaza anti-

Table 1
Simplified lithostratigraphic description of the Taxihe section.

System	Series	Formation	Facies	Lithology	
Quaternary	Pleistocene	Upper part	Wusu Fm (Q ₂ w)	Alluvial Fan	Gray gravels, interbedded with soil-sandstones
		Lower part	Xiyu Fm (Q ₁ x)	Alluvial Fan	Mainly massive gray uncemented conglomerate
Neogene	Pliocene	Upper part	Dushanzi Fm (N ₁₋₂ d)	Fluvial	Gray or brownish sandy mudstone, multi-colored middle-grained sandstone inbedded with thin layers of fine gravel
	Miocene				
Paleogene	Oligocene	Middle part	Taxihe Fm (N ₁ t)	Fluvial	Mainly greenish gray mudstone, brownish sandy mudstone, siltstone and fine-grained sandstone, with some layers interbedding with gypsum and gypsiferous claystones.
		Lower part	Shawan Fm (E ₃ -N ₁ s)	Lacustrine	Mainly reddish or brownish fine-grained mudstone, sandy mudstone, greenish gray marlaceous siltstone, interbedded with gypsiferous claystones
	Eocene	Upper part	Anjihai Fm (E ₂₋₃ a)	Lacustrine	Mainly grayish green mudstones with interbedded thin marlstones, sandstones, shales and layers of gypsum Gastropods, bivalves and ostracods fossils are often found
		Lower part	Ziniquanzi Fm (E ₁₋₂ z)		Mainly gray or gray-brown pebbly sandstone, medium-fine sandstone, interbedded with brown muddy siltstones and mudstone
	Paleocene				

cline (Fig. 2a–d). There, the growth strata show that the main formation time of Kalaza anticline is coeval to the Dushanzi formation (N₁₋₂d).

As shown in the A–B section (Fig. 2a and b), the strata are deformed and eroded intensely, and the strata from Jurassic (J) to Neogene (N₁t) are almost parallel to each other with constant bed thickness, which are interpreted as the pre-growth strata. The strata of the middle Dushanzi formation (N₁₋₂d B) are deposited conformably on the underlying strata at the north limb of the Kalaza anticline but are deposited with an angular unconformably on the deformed Taxihe formation (N₁t) strata at the core of the syncline (also shown in the field pictures Fig. 2c and d). In the north limb, the dips of the Dushanzi formation strata change progressively from 40° in middle part (N₁₋₂d B) to 20° in its upper part (N₁₋₂d C) with decreasing thicknesses towards the fold axis, so here the middle Dushanzi formation is interpreted as representing the deposition of growth strata. In that interval, the deposits change from yellow–gray sandy conglomerates intercalated with sandstones and mudstones to gray or mostly yellow–gray conglomerates with rare mudstones. Together with the growth strata, they suggest important tectonic deformation of the southernmost belt at the time of deposition of the middle Dushanzi formation. Because these sediments of the Kalaza anticline are not directly dated, the age of these growth strata must be estimated using regional correlation of the Dushanzi formation to dated sections. The closest section providing age control on the Dushanzi formation are along the Jingou River and the Taxi river (Fig. 1) indicating respective age ranges 16–7.5 Ma (Charreau et al., 2009a) and ~14–3.0 Ma (Li et al., in press). The large difference in the upper age bound clearly relates to the diachronous nature of the Xiyu conglomeratic formation overlying the Dushanzi formation (Charreau et al., 2009b). Based on these age constraints we infer that observable growth strata observed in the middle Dushanzi formation in the southernmost belt must be older than ~3.0 Ma, probably around ~6 Ma. Indeed, the rock associations of growth strata in the Kalaza anticline is similar to that of the strata in the middle Dushanzi formation with a transition from gray or brownish sandy mudstone, multi-colored middle-grained sandstone to yellow–gray sandy conglomerates and intercalated with sandstones and mudstones dated with an age of ~6 Ma in the Taxihe section based on the magnetostratigraphic age control.

3.2. Growth strata in the middle belt

In the middle belt, close inspection of the exposed stratigraphy in the Taxihe section reveals clear syndepositional deformation within the top of the outcropping Xiyu formation starting at the

~2600 m level in the section (Figs. 1 and 3; see Li et al., in press). These growth strata are defined based on the tapering of beds clearly observed in extensive exposures and can not be associated to simple dip changes on the limb of a fold. Our careful field investigations revealed no other evidence for syntectonic deposition in the Dushanzi formation and lower parts of the section. This is in agreement with reported field observations (Avouac et al., 1993) but contrast with previous interpretations from the Taxihe section arguing for growth strata lower in the Dushanzi formation based mainly on variations in bedding dip attitudes (Lu et al., 2010; Sun and Zhang, 2009). In the Taxihe section, the observed growth strata have been dated with magnetostratigraphy at 2.0 Ma following a clear sediment accumulation increase at ca. 4 Ma in that section (Li et al., in press). Our observations in the Taxihe section thus provide a chronologically consistent sequence of events with increased accumulation rates ca. 4 Ma associated to an advancing thrust front south of the depocenter, followed at 2.0 Ma by folding of the strata expressed by growth strata in the Xiyu formation.

3.3. Growth strata in the northernmost belt

From our field investigations, apparent sedimentary features indicate there are growth strata in Wusu formation on the north limb of Anjihai anticline in the northern belt (Figs. 1 and 4). The conglomeratic Wusu formation angular unconformably overlay on the folded and eroded Dushanzi formation, with the bed thicknesses decreasing towards the fold axis and the bed dips changing from 20° to 5°. These Wusu strata have not been directly dated using magnetostratigraphy. However, age control is provided by magnetostratigraphic dating of the underlying Xiyu formation strata in the Hergosi anticline (Fig. 1) along the Jingou River (Charreau et al., 2009a). In this section, the Xiyu formation is dated up to ~1 Ma. This can be used as a maximum age for the overlying Wusu formation. We thus infer that the growth strata in this northern belt are coeval to the Wusu formation, with a middle Pleistocene age younger than ~1 Ma.

4. Regional structural analysis of seismic profile

To understand the structural deformational styles and magnitude of the anticline belts in the northern edge of Tian Shan Mountain, we provide in the following the structural restoration of a seismic cross profile (Fig. 5 and see Fig. 1 for location). The three paralleled rows of anticline belts have different deformational styles as seen in the seismic profile (Fig. 5). The Qingshuihe anticline in the southernmost belt presents characteristics of basement-involved structural style. Deformation zones within the

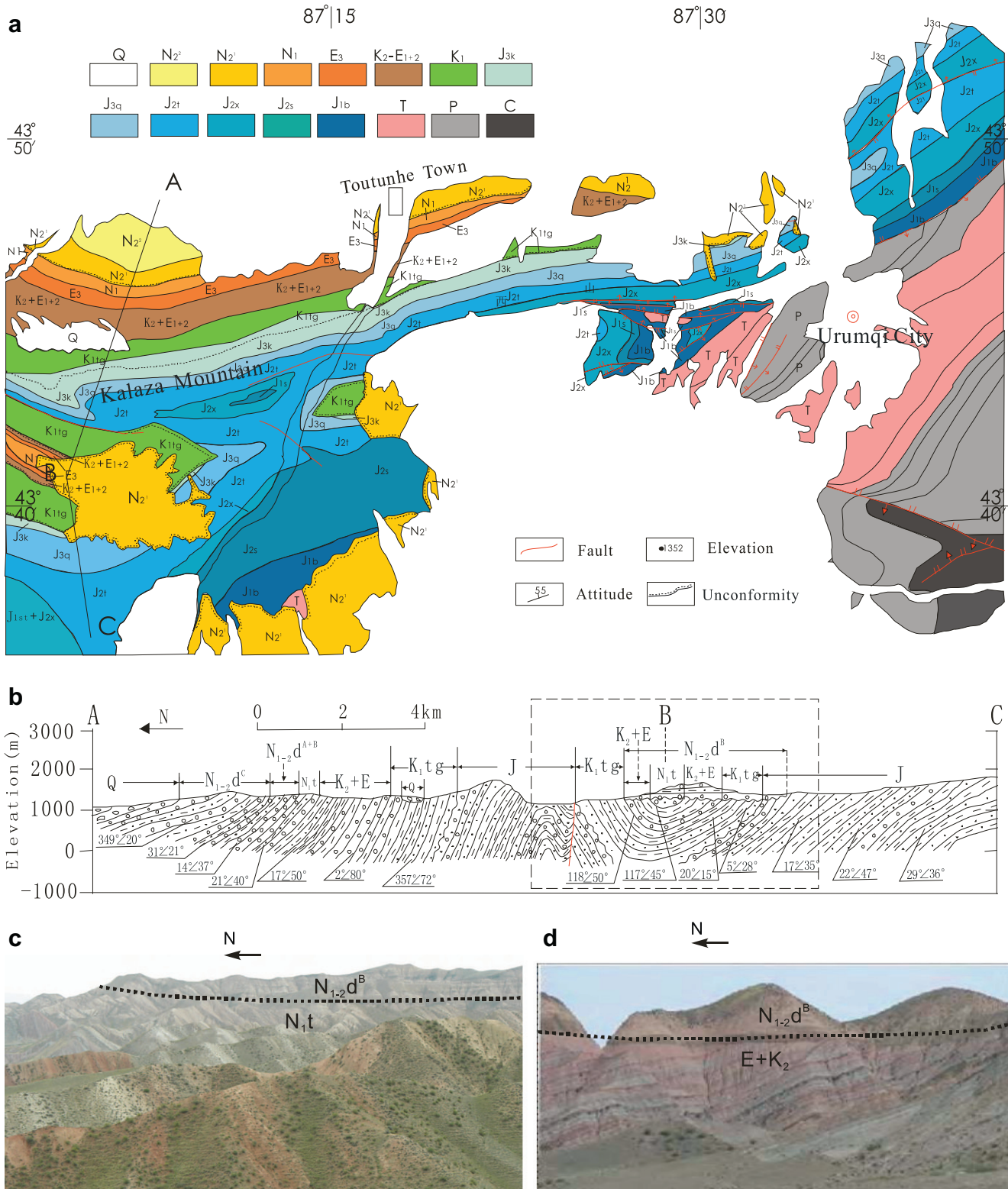


Fig. 2. (a) Geologic map of Kalaza anticline (southern anticlinal belt) and its peripheral area. (b) Schematic section profile of the South–North trending Kalaza anticline. The Dushanzi formation (N₁₋₂d) can be divided here into three units with coarsening upward the lithologies: (I) the lower Dushanzi formation (N₁₋₂d A) consists of brownish yellow massive sandy mudstone and sandy conglomerate, intercalated with fine grained silica sandstone, (II) the middle unit (N₁₋₂d B) is yellow–gray sandy conglomerates and intercalated with sandstones and mudstones, and (III) the upper Dushanzi formation (N₁₋₂d C) is mainly composed of gray or yellow–gray conglomerates. (c) Picture of the southern limb of the Kalaza anticline (southern anticlinal belt).

sedimentary cover dissipate several significant fault slips, with gently dipping front-limbs and back-limbs. Fault slips in the basement are accommodated by a triangular, widening-upward de-

formation zone on the forelimb (trishear) rather than a kink propagation (Almendinger, 1998; Gold et al., 2006). The Huoerguosi anticline in the middle belt indicates a simple fault-bent fold

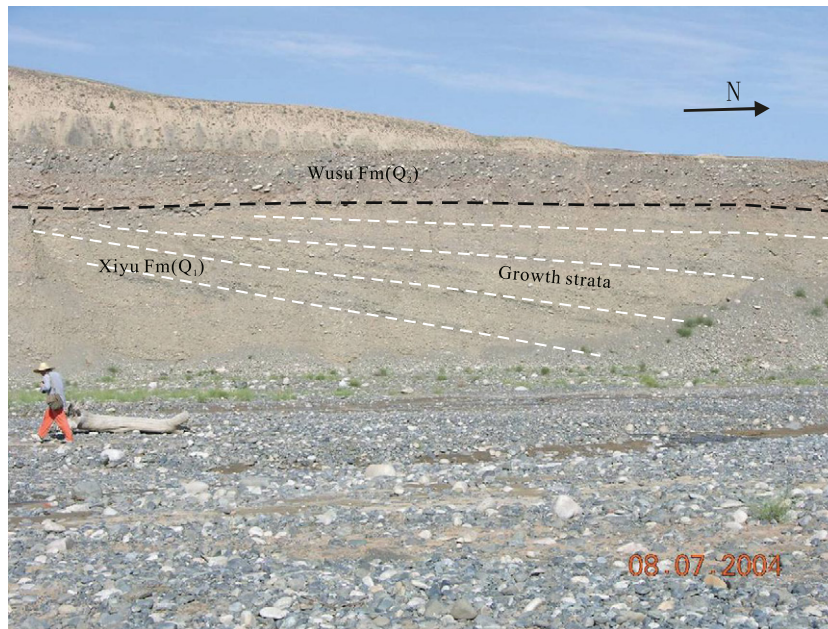


Fig. 3. Growth strata observed in the Taxihe section of the middle anticlinal belt (see Fig. 1 for location), in the upper part of the Xiyu formation and dated at 2.0 Ma (see Li et al., in press).

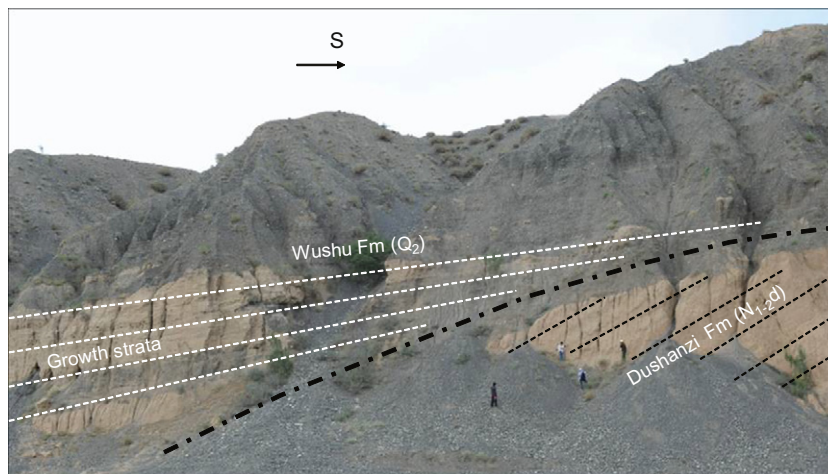


Fig. 4. Growth strata in the Wusu Groups in the northern limb of the Anjihai anticline, northern anticlinal belt (see Fig. 1 for location).

structural style: the reflectors show no significant bed thickness variations and indicate two curved faults ramping up from two subhorizontal décollement layers at the depth of ~ 7.5 km and ~ 3.0 km respectively. The shallower of these faults outcropped the surface and controlled the shapes of the anticline. While the Anjihai anticline of the northern belt has an apparent fault-propagation fold style, almost all the shortening of a flat décollement at depth is absorbed by folding of the overlying stratigraphy similar to trishear fault propagation folding except here the triangle does not contain the extrapolated fault plane as interpreted by Daëron et al. (2007). The interpretation is that most of the deformation associated to the foreland deformation observed in the seismic profile occurred after deposition of the Dushanzi formation and probably continued until Quaternary time, which is consistent with our growth strata observations in the three parallel rows of belts.

Accommodated shortening is quantified from restoration of the balanced cross-section and the timing of deformation is estimated

using evidence for syndepositional deformation in those sections and the strata ages constrained by existing magnetostratigraphic records. The seismic profile is running across anticlinal successions of the Northern Tian Shan foreland. It is a ~ 50 km-long, North–South trending seismic profile (Fig. 5; AB on Fig. 1) running through the Anjihai and Huoerguosi anticlines near the location of the magnetostratigraphically-dated Jingou section (Charreau et al., 2008, 2009a). Well-drilling in the core of these anticlines provided identification of stratigraphic formations and provided parameters for the time–depth construction of the seismic profile. Based on these reconstructions, relatively little variations in formation thicknesses are observed below the Dushanzi formation when compared to the large variations in strata thicknesses above within the Xiyu and the Wusu formations. Using the interpreted seismic profile, structural balancing of cross-section was performed here based on area conservation to calculate the tectonic shortening (Dahlstrom, 1969; Liang et al., 2002). Restoration of the section yields an accommodated shortening of ~ 15 km (22% of restored

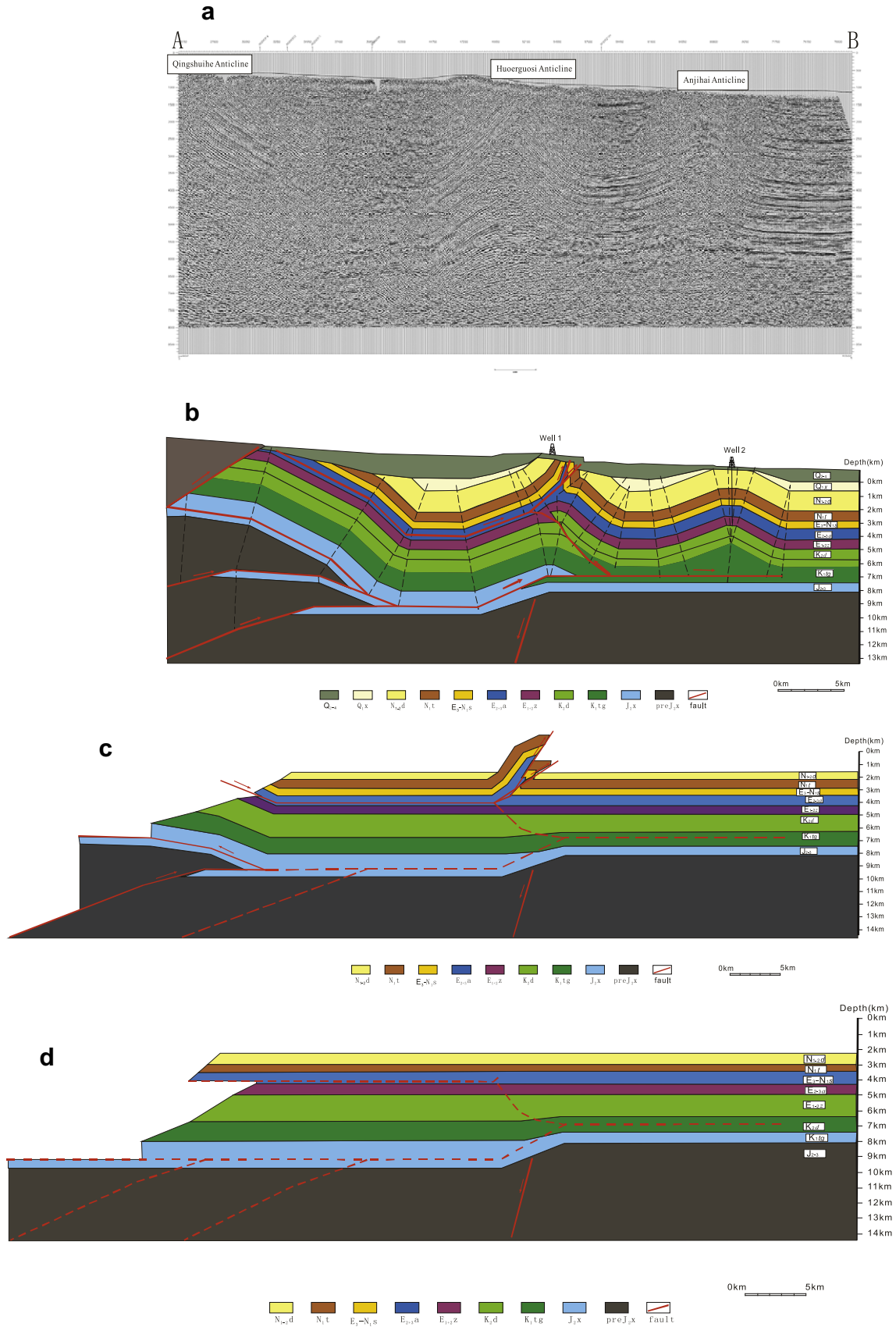


Fig. 5. Interpreted seismic cross-section across the Anjihai and Huoerguosi anticlines and balanced cross-section reconstructions (see AB on Fig. 1 for location). The profile has been constructed with time-depth conversion based on the calibration of well A and well B, and the balanced cross-section was restored with help of the Paradigm's software "GeoSec2D 4.6".

length) across the entire AB section. In excellent agreement with our restoration, these 15 km along the profile can be attributed to 1.55 km folding of the Anjihai anticline in the northern belt (Daëron et al., 2007), ~9.6 km into the Huergosi anticline in the middle belt (Charreau et al., 2008) and ~4 km into the Nananjihai anticline of the southern belt (see review of shortening estimates in Lu et al., 2010).

5. Discussion

5.1. Timing and mechanism of structural deformation

Previous studies have investigated the occurrence of growth strata in order to infer the onset of deformation on the northern Tian Shan fold belts. Initially, observations of growth strata in the outcrop have been used (Lu et al., 2010; Sun and Zhang, 2009) but more recently seismic section analyses have enabled to track down growth structures not necessarily exposed on the surface (Charreau et al., 2008; Daëron et al., 2007).

Interestingly, sub-surface analyses indicate growth strata starting stratigraphically far below observed strata on the surface. Charreau et al. (2008) found growth structures in seismic lines starting at ~10.0 Ma in the Huergosi anticline (middle belt) while we report here the first evidence for tapering of beds at ~2.0 Ma in the Taxi River section of that belt. (Note that suggestions of older growth strata based on changes of dipping attitude only have been reported in sections of the middle belt (Charreau et al., 2009a; Lu et al., 2010; Sun and Zhang, 2009)). Similarly, Daëron et al. (2007) report growth strata starting at 7.4 Ma in the Anjihai anticline (northernmost belt) while we found evidence for growth only above ~1.0 Ma in the Wusu formation. Daëron et al. further showed, based on the geometry of the Anjihai anticline, that the folding was not constant since the onset of the 7.4 Ma growth strata but more likely started slowly and accelerated over the last 0.9 Ma to accommodate most of the deformation. This is in excellent agreement with our growth strata observation in the same Anjihai anticline and suggests that observed growth strata are there reliable indicators of accelerated folding. Daëron et al. observe similar acceleration in other anticlines of the Tian Shan (i.e. the Yakeng anticline in Southern Tian Shan) suggesting this mechanism can be generalized. Based on these considerations, we speculate that the same mechanism can be applied to the middle and southernmost anticlinal belts of the Northern Tian Shan foreland. Consistently, in the middle belt, the deformation would have started slowly at ~10.0 Ma and strongly accelerated at ~2.0 Ma. In the southern belt, seismic evidence is lacking for the onset of slow deformation but accelerated deformation would have started during deposition of the middle Dushanzi formation estimated at ~6 Ma.

5.2. Qualitative shortening rates

Qualitative shortening rate estimates can be made using the ages of anticline formation from growth strata combined with the shortening estimates from our structural restoration of the seismic section. While structures of the southernmost belt are probably mostly inactive in the Quaternary, the Anjihai (northernmost belt) and the Huergosi anticlines (middle belt) are clearly still presently active based on Quaternary terrace offset observations and GPS studies (Avouac et al., 1993; Wang et al., 2001). Long-term rates can thus be obtained for these belts assuming constant rates since the onset of deformation based on the first occurrence of growth structures in the seismic section. This yields 0.2 mm/yr (1.55 km during 7.4 Ma) and 1.0 mm/yr (10 km during 10.0 Ma) for the Anjihai and Huergosi anticlines respectively. However, it

is clear that the shortening rates across both folds accelerated significantly since the onset of folding based on the geometry of these folds and the growth strata observations (Charreau et al., 2008; Daëron et al., 2007). Using the age of onset of the main deformation given by our growth strata observations, we obtain more realistic shortening rate estimates. This yields 1.5 mm/yr (1.55 km during 1.0 Ma) and 5.0 mm/yr (10 km during 2.0 Ma) for the Anjihai and Huergosi anticlines respectively. These must be considered as maximum rates since they also take into account the slow shortening that occurred before the observed growth strata at the surface. They are, however, in excellent agreement with rates previously obtained using other methods (Avouac et al., 1993; Charreau et al., 2008; Daëron et al., 2007) and with GPS-derived North–South rates reported for the Tian Shan at the location of the study area (5.5 ± 1.1 mm/yr at 84.946°E and 44.385°N , station KUYT of Wang et al. (2001); see Fig. 1 for location). This suggests that the rate of deformation in the northern Tian Shan foreland measured from GPS studies and Quaternary slip rates can be extrapolated a few Myrs back.

6. Conclusion

This study provides a regional structural analysis based on identified growth strata dated with magnetostratigraphy and balanced cross sections from interpreted seismic data. Together these data enable to estimate the shortening magnitude and rates across the northern foreland of the Chinese Tian Shan. The three paralleled rows of anticline belts in the northern Chinese Tian Shan have developed in a typical forward-propagated structural pattern from the older southern belt to the younger northern belt. Sub-surface analyses indicate that growth strata start stratigraphically far below observed growth strata on the surface. The latter coincide with – and may therefore be reliable indicators of – accelerated folding. Our results also imply that the northern Tian Shan foreland rates of deformation were lower until late Miocene and increased in more recent times. This provides clues on how the Tian Shan shortening has been partitioned over time and suggests that most of the associated northward motion and the ~7° clockwise rotation of the Tarim block must have occurred in the last few Myrs (Avouac and Tapponnier, 1993; Dupont-Nivet et al., 2002).

Acknowledgements

This study is financially supported by National Basic Research Program of China (2007CB411305 and 2009ZX05009001) and NWO-NSFC programs for G. D.-N. We acknowledge Dr. Li Benliang and Dr. Guan Shuwei at Key Laboratory of Basin Structure & Hydrocarbon Accumulation (Research Institute of Petroleum Exploration & Development) for help with seismic profile interpretation. We thank Prof. An Yin and Prof. Dickson Cunningham for constructive reviews.

References

- Abdrakmatov, K., Aldazhanov, S.A., Hager, B.H., Hamburger, M.W., Herring, T.A., Kalabae, K.B., Makarov, V.I., Molnar, P., Panasyuk, S.V., Prilepin, M.T., Reilinger, R.E., Sadybakasov, I.S., Souder, B.J., Trapeznikov, Y.A., Tsurkov, V.Y., Zubovich, A.V., 1996. Relatively recent construction of the Tien Shan inferred from GPS measurements of present day crustal deformation rates. *Nature* 384, 450–453.
- Almendinger, R., 1998. Inverse and forward numerical modeling of trishear fault propagation folds. *Tectonics* 17, 640–656.
- Avouac, J.P., Tapponnier, P., 1993. Kinematic model of active deformation in central Asia. *Geophysical Research Letters* 20, 895–898.
- Avouac, J.P., Tapponnier, P., Bai, M., You, H., Wang, G., 1993. Active thrusting and folding along the northern Tien Shan and Late Cenozoic rotation of the Tarim relative to Dzungaria and Kazakhstan. *Journal of Geophysical Research* 98, 6755–6804.
- Burbank, D., Meigs, A., Brozovic, N., 1996. Interaction of growing folds and coeval depositional systems. *Basin Research* 8, 199–223.

- Bullen, M.E., Burbank, D.W., Garver, J.L., Abdрахmatov, K.Y., 2001. Late Cenozoic tectonic evolution of the northwestern Tien Shan: new age estimates for the initiation of mountain building. *Geological Society of America Bulletin* 1544, 1559.
- Charreau, J., Chen, Y., Gilder, S., Dominguez, S., Avouac, J.-P., Sen, S., Sun, D., Li, Y., Wang, W., 2005. Magnetostratigraphy and rock magnetism of the Neogene Kuitun He section (northwest China): implications for Late Cenozoic uplift of the Tianshan mountains. *Earth and Planetary Science Letters* 230, 177–192.
- Charreau, J., Gilder, S., Chen, Y., Dominguez, S., Avouac, J.P., Sen, S., Jolivet, M., 2006. Magnetostratigraphy of the Yaha section, Tarim Basin (China): 11 Ma acceleration in erosion and uplift of the Tianshan Mountains. *Geology* 34, 181–184.
- Charreau, J., Avouac, J.P., Chen, Y., Dominguez, S., Gilder, S., 2008. Miocene to present kinematics of fault-bend folding across the Huerquosi anticline, northern Tianshan (China), derived from structural, seismic, and magnetostratigraphic data. *Geology* 36 (11), 871–874.
- Charreau, J., Chen, Y., Gilder, S., Barrier, L., Dominguez, S., Augier, R., Sen, S., Avouac, J.-P., Gallaud, A., Graveleau, F., Wang, Q., 2009a. Neogene uplift of the Tian Shan Mountains observed in the magnetic record of the Jingou River section (northwest China). *Tectonics* 28, TC2008. doi:10.1029/2007TC002137.
- Charreau, J., Gumiaux, C., Avouac, J.-P., Augier, R., Chen, Y., Barrier, L., Gilder, S., Dominguez, S., Charles, N., Wang, Q., 2009b. The Neogene Xiyu Formation, a diachronous prograding gravel wedge at front of the Tianshan: climatic and tectonic implications. *Earth and Planetary Science Letters* 287, 298–310.
- Chen, J., Heermance, R., Burbank, D.W., Scharer, K.M., Miao, J., Wang, C., 2007. Quantification of growth and lateral propagation of the Kashi anticline, southwest Chinese Tian Shan. *Journal of Geophysical Research B: Solid Earth* 112, B03S16. doi:10.1029/2006JB004345.
- Daëron, M., Avouac, J.-P., Charreau, J., 2007. Modeling the shortening history of a fault tip fold using structural and geomorphic records of deformation. *Journal of Geophysical Research* 112, B03S13. doi:10.1029/2006JB004460.
- Dahlstrom, C.D.A., 1969. Balanced cross section. *Canadian Journal of Earth Sciences* 6, 743–757.
- Dupont-Nivet, G., Guo, Z., Butler, R.F., Jia, C., 2002. Discordant paleomagnetic direction in Miocene rocks from the central Tarim Basin: evidence for local deformation and inclination shallowing. *Earth and Planetary Science Letters* 199, 473–482.
- Deng, Q., Feng, X., Zhang, P., Xu, X., Yang, X., Peng, S., Li, J., 2000. Active Tectonics of the Tian Shan Mountains. Seismology Press, Beijing, p. 399.
- Gao, J., Klemm, R., 2003. Formation of HP–LT rocks and their tectonic implications in the western Tianshan Orogen, NW China: geochemical and age constraints. *Lithos* 66, 1–22.
- Gold, R.D., Cowgill, E., Wang, X.-F., Chen, X.-H., 2006. Application of trishear fault-propagation folding to active reverse faults: examples from the Dalong Fault, Gansu Province, NW China. *Journal of Structural Geology* 28, 200–219.
- Han, B., Guo, Z., Zhang, Z., Zhang, L., Chen, J., Song, B., 2010. Age, geochemistry, and tectonic implications of a late Paleozoic stitching pluton in the North Tian Shan suture zone, western China. *GSA Bulletin* 122 (3/4), 627–640. doi: 10.1130/B26491.1.
- Hardy, S., Poblet, J., 1994. Geometric and numerical model of progressive limb rotation in detachment folds. *Geology* 22 (4), 371–374.
- Heermance, R.V., Chen, J., Burbank, D.W., Wang, C., 2007. Chronology and tectonic controls of late tertiary deposition in the southwestern Tian Shan foreland, NW China. *Basin Research* 19, 599–632.
- Huang, B., Piper, J.D.A., Peng, S., Liu, T., Li, Z., Wang, Q., Zhu, R., 2006. Magnetostratigraphic study of the Kuche Depression, Tarim Basin, and Cenozoic uplift of the Tian Shan Range, Western China. *Earth and Planetary Science Letters* 251, 346–364.
- Li, C., Dupont-Nivet, G., Guo, Z., in press. Magnetostratigraphy of the Northern Tian Shan foreland, Taxi He section, China. *Basin Research*. doi: 10.1111/j.1365-2117.2010.00475.x.
- Li, J., 2006. Permian geodynamic setting of Northeast China and adjacent regions: closure of the Paleo-Asian Ocean and subduction of the Paleo-Pacific Plate. *Journal of Asian Earth Sciences* 26, 207–224.
- Liang, H., Zhang, J., Xia, Y., 2002. The balanced Section Technique and its Application in the Petroleum Exploration. Seismology Press, Beijing, 12–22.
- Lu, H., Burbank, D.W., Li, Y., Yunming, Liu, 2010. Late Cenozoic structural and stratigraphic evolution of the northern Chinese Tian Shan foreland. *Basin Research* 22, 249–269.
- Molnar, P., England, P., Martinod, J., 1993. Mantle dynamics, uplift of the Tibetan Plateau, and the Indian monsoon. *Reviews of Geophysics* 31, 357–396.
- Scharer, K.M., Burbank, D.W., Chen, J., Weldon II, R.J., 2006. Kinematic models of fluvial terraces over active detachment folds: constraints on the growth mechanism of the Kashi-Atushi fold system, Chinese Tian Shan. *Bulletin of the Geological Society of America* 118, 1006–1021.
- Shu, L., Yu, J., Charvet, J., Laurent-Charvet, S., Sang, H., Zhang, R., 2004. Geological, geochronological and geochemical features of granulites in the Eastern Tianshan, NW China. *Journal of Asian Earth Sciences* 24, 25–41.
- Sobel, E.R., Chen, J., Heermance, R.V., 2006. Late Oligocene–Early Miocene initiation of shortening in the Southwestern Chinese Tian Shan: implications for neogene shortening rate variations. *Earth and Planetary Science Letters* 247, 70–81.
- Sun, J., Zhu, R., Bowler, J., 2004. Timing of the Tianshan Mountains uplift constrained by magnetostratigraphic analysis of molasse deposits. *Earth and Planetary Science Letters* 219, 239–253.
- Sun, J., Xu, Q., Huang, B., 2007. Late Cenozoic magnetostratigraphy and paleoenvironmental changes in the northern foreland basin of the Tian Shan Mountains. *Journal of Geophysical Research* 112. doi:10.1029/2006JB004653.
- Sun, J., Zhang, L., Deng, C., Zhu, R., 2008. Evidence for enhanced aridity in the Tarim Basin of China since 5.3 Ma. *Quaternary Science Reviews* 27, 1012–1023.
- Sun, J., Zhang, Z., 2009. Syntectonic growth strata and implications for late Cenozoic tectonic uplift in the northern Tian Shan, China. *Tectonophysics* 463, 60–68.
- Suppe, J., Chou, G.T., Hook, S.C., 1992. Rates of Folding and Faulting Determined from Growth Strata. In: McKelvey, K.R. (Ed.), *Thrust Tectonics*. Chapman and Hall, London, pp. 105–121.
- Tapponnier, P., Molnar, P., 1979. Active faulting and Cenozoic tectonics of the Tien Shan, Mongolia, and Baykal regions. *Journal of Geophysical Research* 84, 3425–3459.
- Wang, Q., Zhang, P., Freymueller, J.T., Bilham, R., Larson, K.M., Lai, X.a., You, X., Niu, Z., Wu, J., Li, Y., Liu, J., Yang, Z., Chen, Q., 2001. Present-day crustal deformation in China constrained by global positioning system measurements. *Science* 294, 574–577.
- Windley, B.F., Allen, M.B., Zhang, C., Zhao, Z., Wang, G., 1990. Paleozoic accretion and Cenozoic reformation of the Chinese Tien Shan Range, central Asia. *Geology* 18, 128–131.
- Xiao, W., Windley, B.F., Yuan, C., Sun, M., Han, C., Lin, S., Chen, H., Yan, Q., Liu, D., Qin, K., Li, J., Sun, S., 2009. Paleozoic multiple subduction-accretion processes of the southern Altai. *American Journal of Science* 309, 221–270.
- Yin, A., Nie, S., Craig, P., Harrison, T.M., Ryerson, F.J., Qian, X., Yang, G., 1998. Late Cenozoic tectonic evolution of the southern Chinese Tian Shan. *Tectonics* 17, 1–27.